

Supplemental Materials

Molecular Biology of the Cell

Berends et al.

Supplemental Figure Legends

Supplementary figure 1: Cortical actin filaments inhibit anterior pulling forces during mitosis of the one-cell embryo. (A) Spindle elongation in permeabilized embryos either treated with cytochalasin D, or solvent only (control). Average values (\pm SD). (B) Time-lapse images of both spindle poles from NEBD till late anaphase. In control embryos, the posterior spindle pole flattens at the end of anaphase (arrow). Note that the posterior spindle pole does not flatten in embryos treated with latrunculin A or cytochalasin D (arrows).

Supplementary figure 2: PAR-2::GFP remains restricted to the posterior domain in the absence of filamentous actin. A) PAR-2::GFP localization in an untreated embryo (Control, top), *perm-1(RNAi)* embryo (middle) and *perm-1(RNAi)* embryo exposed to cytochalasin D (bottom). Time is in minutes after nuclear envelope breakdown (NEBD). B) Cell surface domain occupied by PAR-2::GFP. The boundary between absence and presence of PAR-2::GFP is expressed as % embryo length measured from the anterior end. n=12 (control, left), 7 (*perm-1(RNAi)* middle) or 8 (*tcc-1(RNAi)* +cytoD right) C) Quantification of PAR-2::GFP fluorescence. Line scan analysis of the fluorescence of peripheral PAR-2::GFP from images as in (A) (see Material and methods for details)

Supplementary figure 3: GOA-1 contributes more prominently to spindle pole oscillations and cortical invaginations than GPA-16. (A) Maximum amplitudes of spindle pole oscillations during anaphase. Average values (\pm SD) of the anterior and posterior spindle poles are shown for the indicated genotypes (n \geq 7). (B) Cortical invaginations visualized by FM 1-43FX membrane staining in a control embryo treated with cytochalasin D (arrows, left panel). Quantification of cortical invaginations observed during anaphase in N2, *gpa-16(ok2349)*, and *goa-1(sa734)* embryos treated with cytochalasin D (right panel). Average values are indicated (\pm SD, n \geq 9). See *Materials and Methods* for details.

Supplementary figure 4: Spindle elongation during the first mitotic division of zygotes with the indicated genotypes. Horizontal: time indicated from nuclear envelope breakdown (NEBD) onward. Vertical: distance between spindle poles, expressed as percentage of embryo length. Average values \pm SD, n \geq 7.

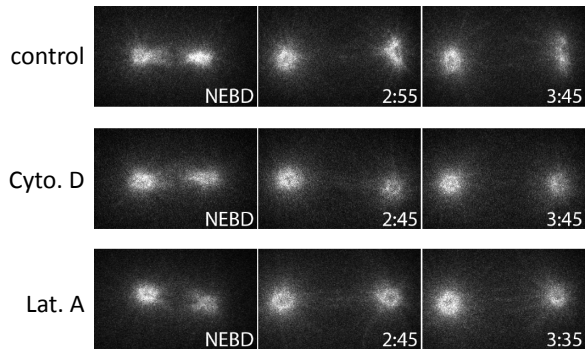
Supplementary figure 5: TCC-1 is not required for asymmetric positioning of the cell cleavage plane. Time-lapse series of a control embryo (left two panels), and *tcc-1* RNAi treated embryo (right two panels). Embryos express *mCherry::tbg-1* and *mCherry::H2B*, to visualize the position of the centrosomes (white arrowheads) and DNA (arrow), respectively. Pb: polar body. Note the normal asymmetric position of the cleavage plane (red arrowhead) in the *tcc-1* (RNAi) embryo.

Supplementary figure 6: Loss of TCC-1 in the embryo does not result in altered GOA-1 and LIN-5 levels at the cortex. (A) Control and *tcc-1(RNAi)* embryos stained for GOA-1, LIN-5 and DNA (DAPI). Note that GOA-1 and LIN-5 localization is similar at the plasma membrane in *tcc-1(RNAi)* and control embryos (arrows and arrowheads). Quantification of cortical GOA-1 (B) and LIN-5 (C) enrichment, measured at the contact between the AB and P2 blastomeres. Average values (\pm SD) are indicated, N2: n=17, *tcc-1(RNAi)*: n=33.

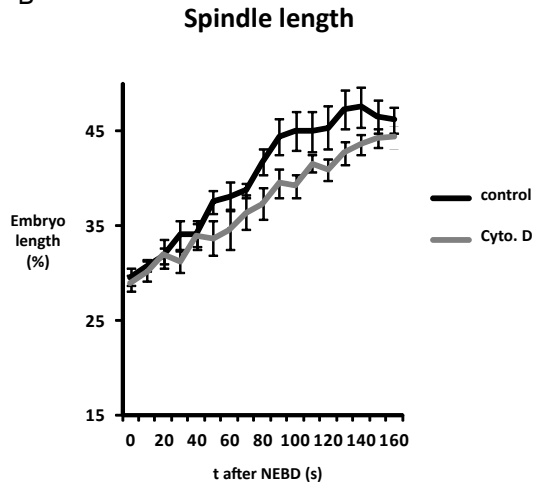
Supplementary figure 7: TCC-1 contributes to meiotic spindle translocation, but not meiotic spindle rotation. Depicted are still images from time-lapse recordings of *lin-5(RNAi)*, *tcc-1(RNAi)+unc-116(RNAi)*, and *tcc-1(RNAi)+lin-5(RNAi)* embryos. Note that the dynein dependent meiotic spindle rotation (arrow and arrowhead) does not occur after *lin-5* RNAi (second and bottom panels), while it does occur in *tcc-1(RNAi)+unc-116(RNAi)* embryos (arrowhead, top row). See supplementary movies for further details.

Supplementary figure 8: UNC-116 has a weak dampening effect on spindle pole oscillation. (A) Maximum amplitudes of spindle pole oscillations in control RNAi-treated normal embryos (N2) versus *unc-116(RNAi)* embryos. (A) Average values of the anterior and posterior spindle poles (\pm SD), (B) values as measured in individual embryos. Anterior pole rocking is significantly different between N2 and *unc-116* RNAi ($P < 0,02$).

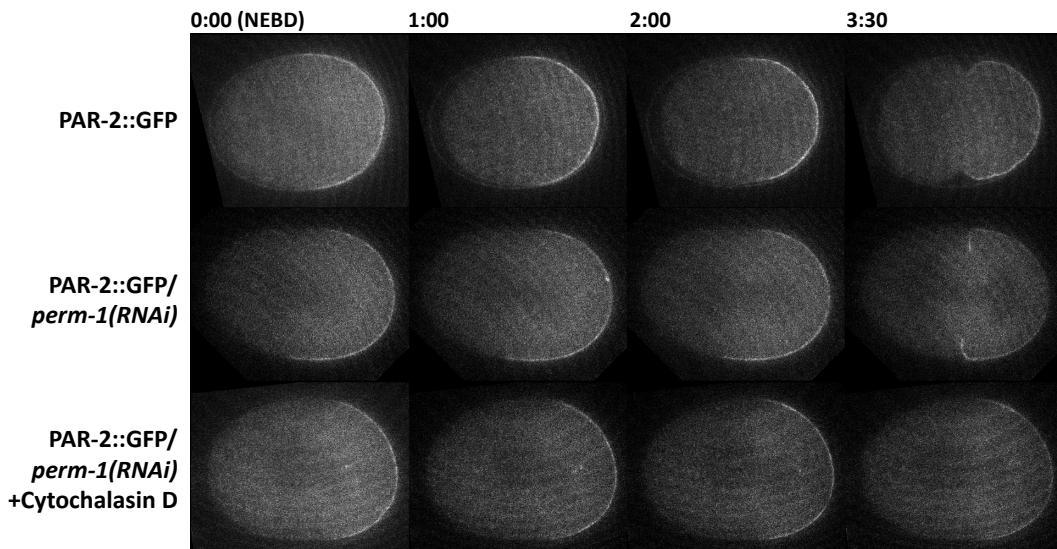
A



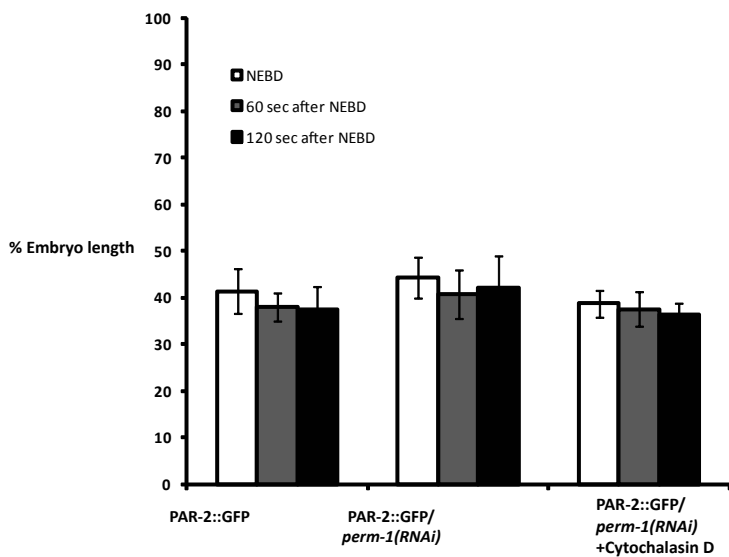
B



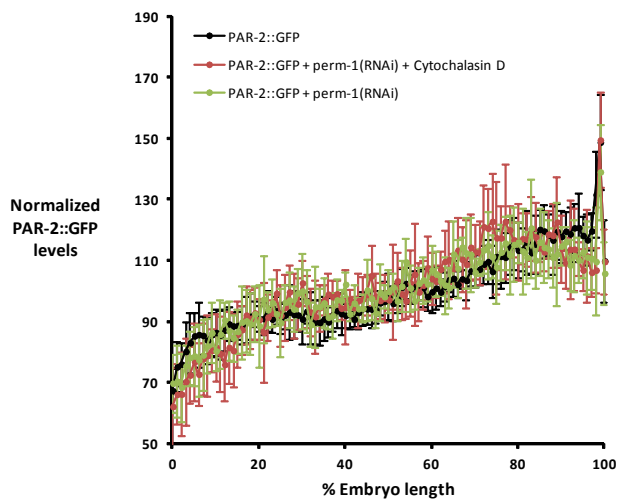
A



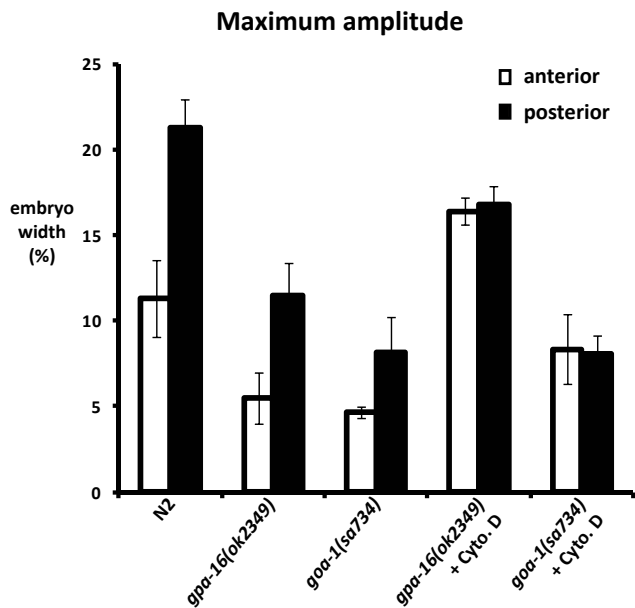
B



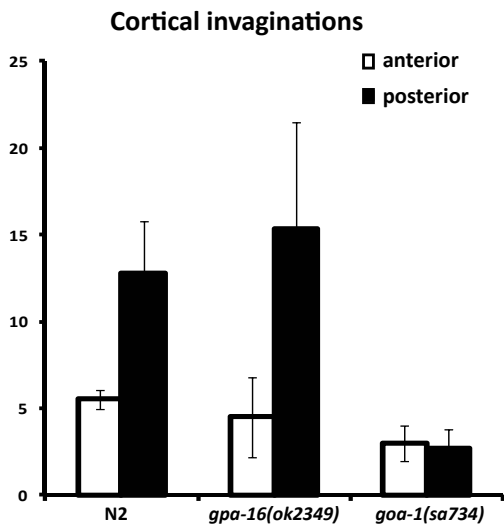
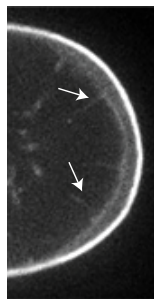
C



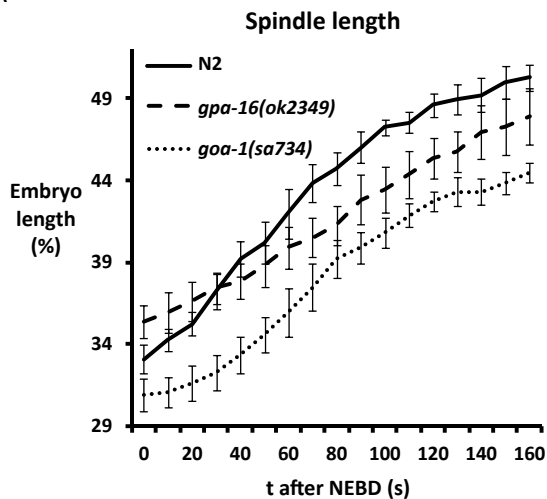
A



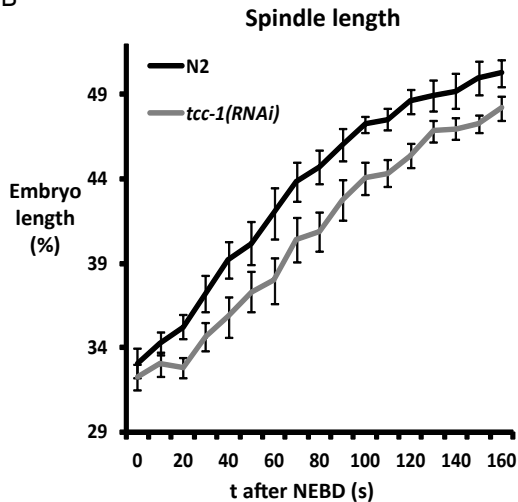
B



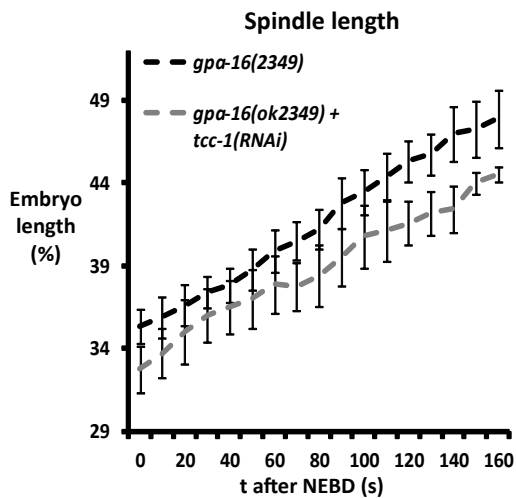
A



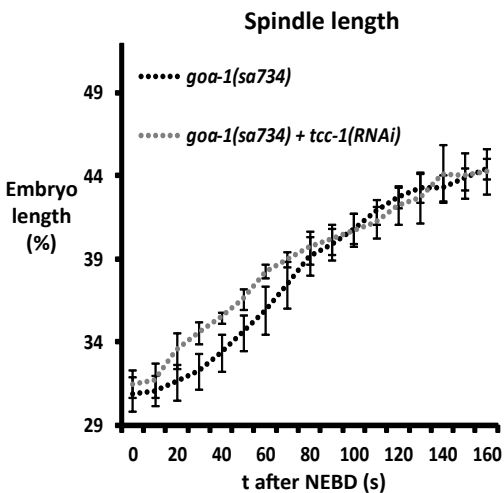
B

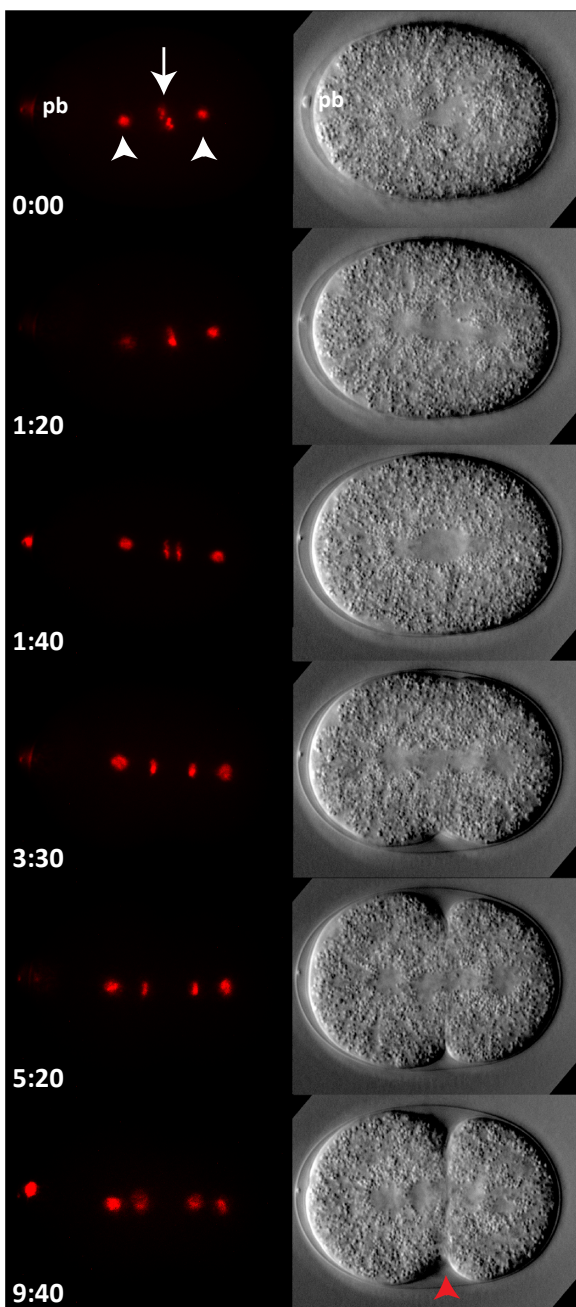
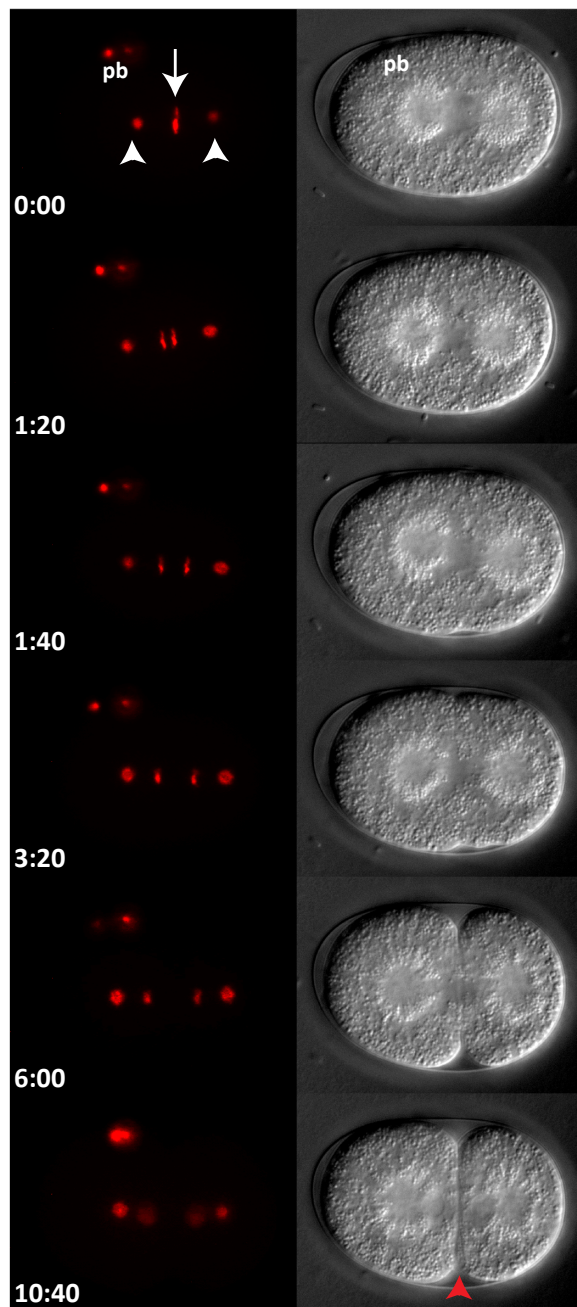


C

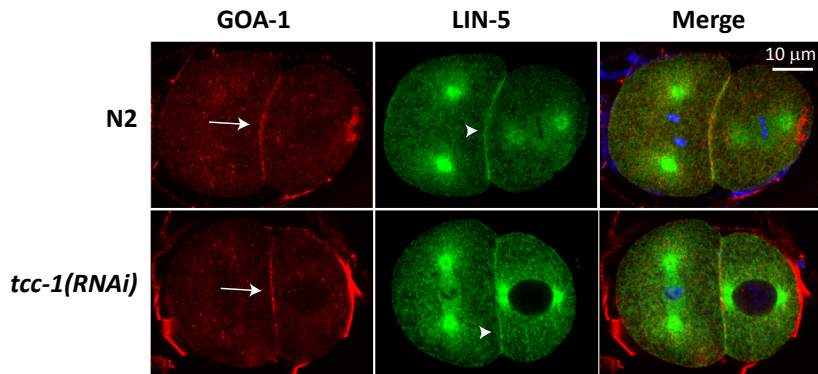


D



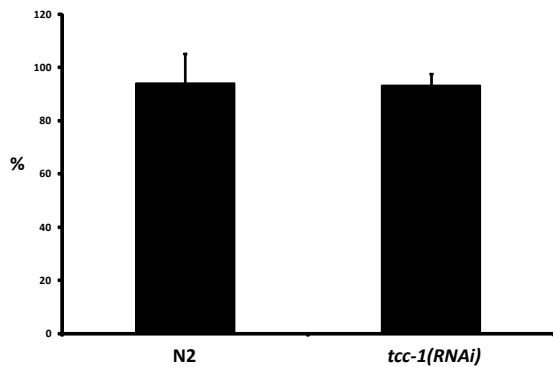
N2***tcc-1(RNAi)***

A



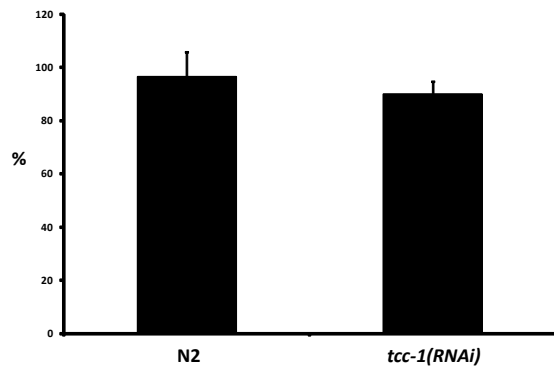
B

Cortical GOA-1 enrichment

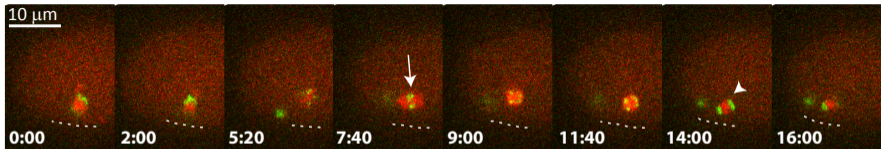


C

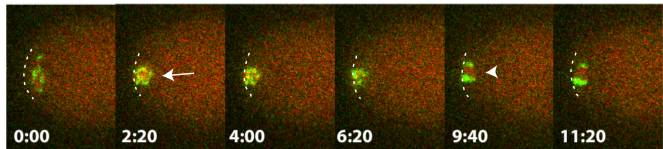
Cortical LIN-5 enrichment



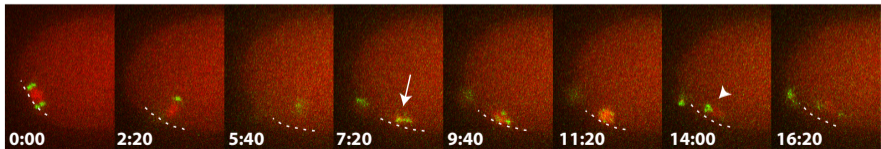
tcc-1(RNAi)+unc-116(RNAi)



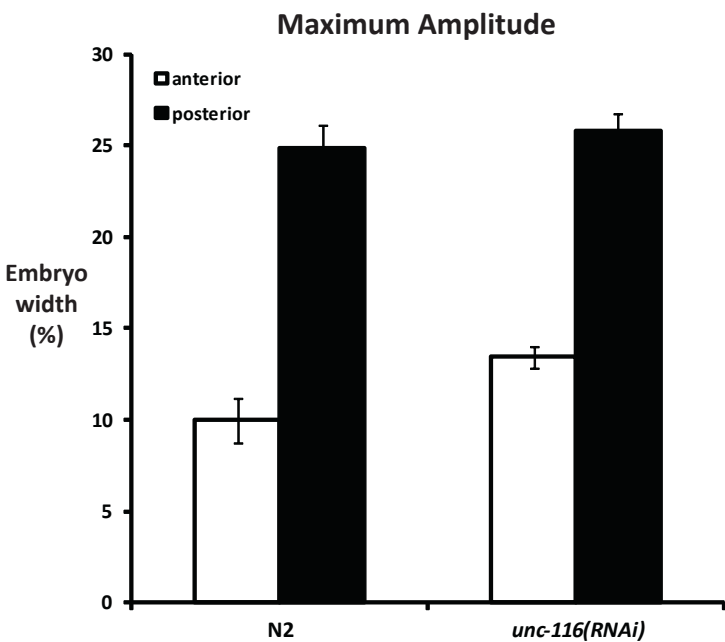
lin-5(RNAi)



tcc-1(RNAi)+lin-5(RNAi)



A



B

